Available online at website: https://journal.bcrec.id/index.php/bcrec

Bulletin of Chemical Reaction Engineering & Catalysis, 19 (3) 2024, 384-392

Research Article

Gelatin's Effect on Iron Oxide Nanoparticle Properties and Its Use in Thermal Regeneration for Methylene Blue Photodegradation

Maria Ulfa*, Shabrina Devinta Poetry

Chemistry Education Study Program, Faculty of Teacher Training and Education, Sebelas Maret University, Jl. Ir. Sutami 36A, Surakarta 57126, Indonesia.

Received: 18th June 2024; Revised: 1st August 2024; Accepted: 1st August 2024
Available online: 7th August 2024; Published regularly: October 2024

Abstract

Two series of iron oxide nanoparticles with different textural and structural characteristics were synthesized using the sol-gel method. The iron oxide nanoparticles were made with synthetic (Pluronic P123 Amphiphilic Block Copolymer) and natural (gelatin) double templates and single P123 templates. The influences of the addition of the gelatin template on the microstructure, methylene blue degradation, and thermal photocatalyst regeneration were investigated. The X-ray Diffraction (XRD) examination revealed the formation of iron-P123-gelatin (iron oxide made with P123 and gelatin templates) and iron-P123 (iron oxide made with only P123 template) with hematite and maghemite phases, where the crystallinity and crystallite size increased due to the presence of gelatin. Fourier Transform Infra Red (FTIR) studies indicated a peak at 500 cm^{-1}, revealing the iron groups in both samples and increased intensity in the hydroxyl and carbonyl groups due to gelatin. Furthermore, the surface area, pore volume, and pore diameter of iron-P123-gelatin exhibited an increment due to gelatin addition. According to the Thermogravimetric Analysis (TGA) and Differential Thermal Analyzer (DTA) data, the sample with gelatin had higher thermal stability and weight loss than that without gelatin. The photodegradation of methylene blue utilizing iron-P123-gelatin reached 91.5%, showing a better performance than that of iron-P123. Finally, iron-P123-gelatin demonstrated a promising photocatalyst thermal regeneration for methylene blue photodegradation for 5 cycles at various temperatures, and it is suggested that 450 °C was the ideal temperature.

Keywords: iron oxide; nanoparticles; gelatin; P123; photocatalyst; methylene blue; photodegradation; regeneration

How to Cite: M. Ulfa, S.D. Poetry (2024). Gelatin's Effect on Iron Oxide Nanoparticle Properties and Its Use in Thermal Regeneration for Methylene Blue Photodegradation. *Bulletin of Chemical Reaction Engineering & Catalysis*, 19 (3), 384-392 (doi: 10.9767/bcrec.20172)

Permalink/DOI: https://doi.org/10.9767/bcrec.20172

Introduction

Nowadays, the textile industry generates enormous amounts of wastewater, including hazardous dyes such as methylene blue [1-3]. Methylene blue waste from the textile industry should be handled before being disposed of in the environment since it has genotoxic and mutagenic effects that are harmful to living beings [4-6]. Advanced Oxidation Processes (AOPs) are acknowledged as an efficient technology for treating wastewater that poses an environmental risk. Among these, photocatalysis has received a lot of attention because of its considerable influence on environmental pollution and the worldwide energy crisis. Photocatalysis is a low-cost, effective, and ecologically friendly technology for removing dangerous contaminants that rely on light rather than chemicals. Refractory organic pollutants have been shown to be totally mineralized and successfully decomposed by this less energy-intensive and environmentally friendly technique.

One well-known method of photocatalysis is photocatalytic photodegradation, which has become a highly efficient way of eliminating methylene blue dye from wastewater [3,7-10]. Still, the process requires photocatalysts to promote a chemical reaction so that

* Corresponding Author.
Email: mariaulfa@staff.uns.ac.id (M. Ulfa)

photodegradation can occur [2,11,12]. Currently, researchers are interested in nanoparticles for photocatalysts, and several strategies have been developed to increase the material's effectiveness in methylene lue dye waste degradation.

In particular, iron oxide nanoparticles are a nontoxic inorganic substance extensively studied as one of the photocatalysts for dye photodegradation due to their fascinating properties [13-16]. The size of iron oxide nanoparticles is about 2-50 nm, and accompanied by their homogeneous particle shapes and surfaces, they allow them to interact easily with organic molecules, such as methylene blue, resulting in excellent photocatalytic performance [14,17,18].

Iron oxide nanoparticles can be synthesized via sol-gel, arc-discharge, micro-emulsion, thermal decomposition, hydrothermal synthesis, ball milling, and co-precipitation methods [2,11,17,19,20]. Nevertheless, a green templating technique has attracted attention to the preparation of iron oxide nanoparticles [19]. The P123, F127, cetyltrimethylammonium bromide, and cetyltrimethylammonium chloride can be employed as synthetic structure-directing agents [16,21]. Still, their usage can be minimized by replacing them with biodegradable natural reagents, such as plant extracts. The use of plant extracts can produce nanoparticles in various forms [11,21]. However, their utilization also has a negative impact, as it results in residual by-products in the synthesized materials that can interrupt their characterization and application processes [19]. Plant extract can be replaced with an extract from animals, such as gelatin, which can be derived from the hydrolysis of animal skin and bone waste [22,23]. Additionally, gelatin has a reasonably stable amine group that can form a solid affinity with precursor as pore director in the molecular rearrangement process [23,24].

The combination of structure-directing agents, especially the P123 synthetic template and gelatin organic template, for the synthesis of iron oxide nanoparticles photocatalysts has never been reported, which became the novelty of this research. Therefore, this study aimed to synthesize iron oxide nanoparticles using the sol-gel method and a combination of P123 and gelatin templates. This study further investigated the influences of the gelatin template on the structural and textural properties and methylene blue photodegradation. Furthermore, the thermal regeneration of the synthesized iron oxide photocatalysts for methylene blue photodegradation was examined at various temperatures.

2. Experimentals

2.1 Material

The materials were HCl 37% (Mr = 36.5 g/mol), gelatin (Mr = 90.000 g/mol), pluronic P123 (Mr = 5800 g/mol), iron nitrate ($Fe(NO_3)_3.9H_2O$) 98% (241.86 g/mol), pure water (18 g/mol), and methylene blue (319.85 g/mol). All reagents were purchased from Sigma Aldrich.

2.2 Synthesis of Iron Oxide Nanoparticles

An amount of 4 g of P123 was mixed with 19.5 mL of 37% HCl, 127 mL of distilled water, 0.0861 g of 1% agar, 0.431 g of 5% agar, 0.861 g of 10% gelatin, 1.723 g of 20% agar, and 16.83 g of iron nitrate (Solution 1). Separately, 19.5 mL of 37% HCl was diluted in 127 mL of distilled water (Solution 2). Then, the Solution 1 was mixed with Solution 2 using a magnetic stirrer under closed conditions at 500 rpm and 40 °C (Solution 3). After that, 16.83 g of iron nitrate was added to Solution 3 and stirred at the same speed and temperature for 24 hours. The resulting final solution was then placed in a hydrothermal autoclave (Trident Labortek) and heated at 90 °C for 24 h. Afterward, it was rinsed using 20 mL of 5 M NaOH until the pH was neutral and a residue was produced. The residue was then heated in an oven at 100 °C for 24 h to obtain powder samples. The powder was crushed using a mill and pestle until the smooth and fine particles were obtained. Finally, the powder samples were calcined in a furnace (HPE) at 550 °C for 5 h. The resulting samples were then labeled as Iron-P123-gelatin and Iron-P123 for the samples with and without gelatin template, respectively.

2.3 Characterizations

The samples were analyzed using the XRD Pananalytica Version PW3050/60 instrument with CuKα radiation (1.5418 Å) with an angle range of 10° – 80° to analyze their crystal orientation. The shape and particle sizes of the samples were investigated using Tescan Mira3 SEM-Czechia SEM. The UV-Vis transmission spectra of the iron oxide samples were measured using a double-beam spectrophotometer (UV-1800, Shimadzu) in the 200-900 nm range. The function group and vibration modes were explored using Fourier transform infrared spectrum (FTIR) by Spectrum GX FT-IR (Perkin Elmer) with a potassium bromide (KBr) beam splitter.

2.4 Iron-P123-gelatin for Degradation of Methylene Blue under Light Irradiation

To test the photocatalytic activity of the Iron-P123-gelatin sample, 5 mg of methylene blue was mixed into 1000 mL of deionized water to achieve

a final concentration of 5 mg/L. Then, 50 mg of the powder samples were dispersed into the methylene blue solution. The 200 mL of the mixed solution was agitated for 10 min by stirring with a magnetic stirrer in the dark to keep the iron-P123-gelatin and iron-P123 suspensions at equilibrium. After that, the mixture was exposed to a visible light source at 660 nm (63 mW/mm^2, as measured by an SM 206 solar power meter) for 60 min at a distance of 1.3 m. Finally, around 4 mL of the irradiated samples were taken every 10 min and measured using UV-vis spectrophotometry (Shimadzu, UV 1800) to obtain the absorbances. From the absorbance data, the % photodegradation efficiency of methylene blue (% Efficiency) could be calculated using Equation 1. In which C_0 and C_t are the initial concentration and the concentration at t time, respectively.

$$\%Efficiency = \frac{C_0 - C_t}{C_0} \times 100\% \quad (1)$$

3. Result and Discussion

Figure 1 denotes the XRD patterns of the samples of iron oxide nanoparticles with P123-gelatin and P123 templates. It reveals that, with and without gelatin, both samples have significant peaks of iron oxide hematite (α-Fe_2O_3) according to JCPDS No. 79-0007 [15,16,20]. The other peaks demonstrating maghemite (γ-Fe_2O_3) were observed, meaning the hybrid phase character of the products. It seems that the hematite would likely have a preferred growth orientation along the (104) direction (31.61°) for the sample with gelatin if the (104) diffraction peak intensity were stronger than the (110) direction (35.62°).

On the other hand, Table 1 demonstrates that the crystallinity of the iron oxide samples with the gelatin template increased from 67% to 90%. This is purportedly because the twofold templating effect (P123-gelatin) enhanced the rearrangement points of iron atoms. This is also supported by the characteristic peaks at 23.74°, 31.61°, and 35.62° linked to an increase in the hematite Fe_2O_3 peak. The results also denote that the use of multiple templates yields a massive rearrangement of the iron oxide precursor's atoms, printing each remaining iron atom in a more uniform framework than would be possible with a single template. Therefore, the presence of gelatin causes an increase not only in the crystallinity but also in the crystallite size of iron oxide, where the broadening of the diffraction peaks observed is consistent with the involvement of gelatin. This can advance the crystallization and crystallite size expansion of iron oxide because the strong interaction between the amine group and the iron ion causes an increase in the molecular density of the iron precursor [6].

The FTIR analysis was done to identify the functional groups involved in the iron oxide samples (Figure 2). For the spectrum of the iron-P123-Gelatin sample, relatively prominent peaks about 3450 cm^{-1} and 1640 cm^{-1} represent the existence of hydroxyl functional groups. The peak at about 1470 and 2200 cm^{-1} is associated with the

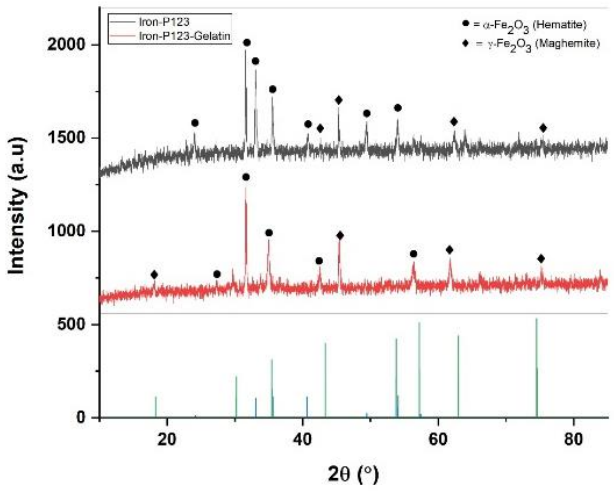

Figure 1. XRD patterns of iron oxide nanoparticles prepared with P123-gelatin and P123 templates.

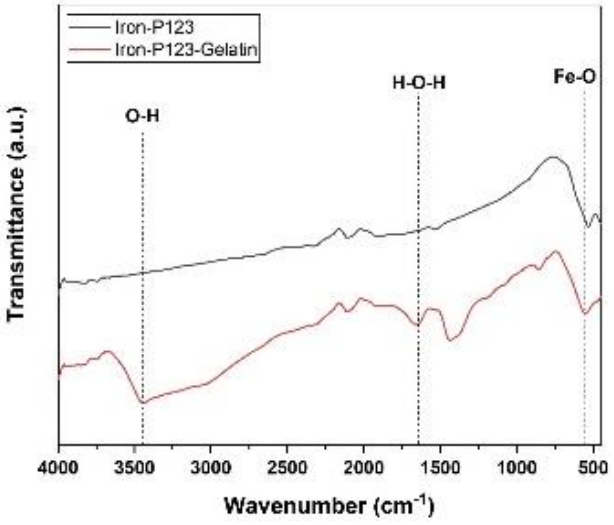

Figure 2. FTIR spectra of iron oxides with and without gelatin.

Table 1. Structural property of iron oxide nanoparticles made with and without gelatin.

Sample	Main peak 2θ (°)	Crystallite size (nm)	Crystallinity (%)
Iron-P123	31.61	18.13	67
Iron-P123-Gelatin	31.64	97.92	90

presence of the carbonyl group. Meanwhile, the peak at around 500 cm^{-1} indicates the formation of iron groups (Fe–O). At the spectrum of iron-P123 (without gelatin), the peak at about 2222 cm^{-1} denotes the C–O–C bond. The significant peak at around 500 cm^{-1} points to the iron group (Fe–O). The addition of gelatin onto iron oxide during synthesis was revealed by the change of the peak at 3450 cm^{-1} and 1470 cm^{-1}. The peak at 3450 cm^{-1} corresponding to the rich O–H functional group might be due to the strong interaction of the amine group of gelatin to attract iron and oxygen. Meanwhile, the peak at 1470 cm^{-1} corresponding to the carbonyl group is considered due to the presence of the amine group of gelatin. Figure 3 presents morphology images and particle size distributions of iron oxides with and without gelatin.

The nitrogen adsorption-desorption isotherms were investigated to measure the pore structure of the prepared samples. Figures 4 and 5 show the curves of nitrogen adsorption-desorption isotherms and pore volumes of the iron oxide nanoparticles, respectively. According to Figure 4, the curve of the iron-P123-gelatin sample reveals a prominent hysteresis loop, demonstrating that the sample has a mesoporous structure [21,25]. Furthermore, based on Figure 5, the mesoporous size for iron oxide P123-gelatin peaked at 13.5 nm, which is a significant increase from that of the iron-P123 (without gelatin) sample (3.2 nm). The iron-P123 (without gelatin) sample exhibits maximum nitrogen uptake in a single layer at low pressure so that there is a sharp increase in the curve approaching P/P0<1 (Figure 3). In contrast, in the mesoporous layer, initially, single-layer coverage occurs, followed by multiple and successive layers filling capillary condensation [6]. However, as the broader mesopores, more significant pressure is required to fill them because multilayer adsorption occurs at low-energy locations (bilayers) far from the walls. Therefore, maximum nitrogen adsorption/desorption occurs in high-pressure areas. Thus, hysteresis shifts towards high P/P0 areas (> 0.6) so that the pore size of the iron-P123-gelatin reaches 13.5 nm.

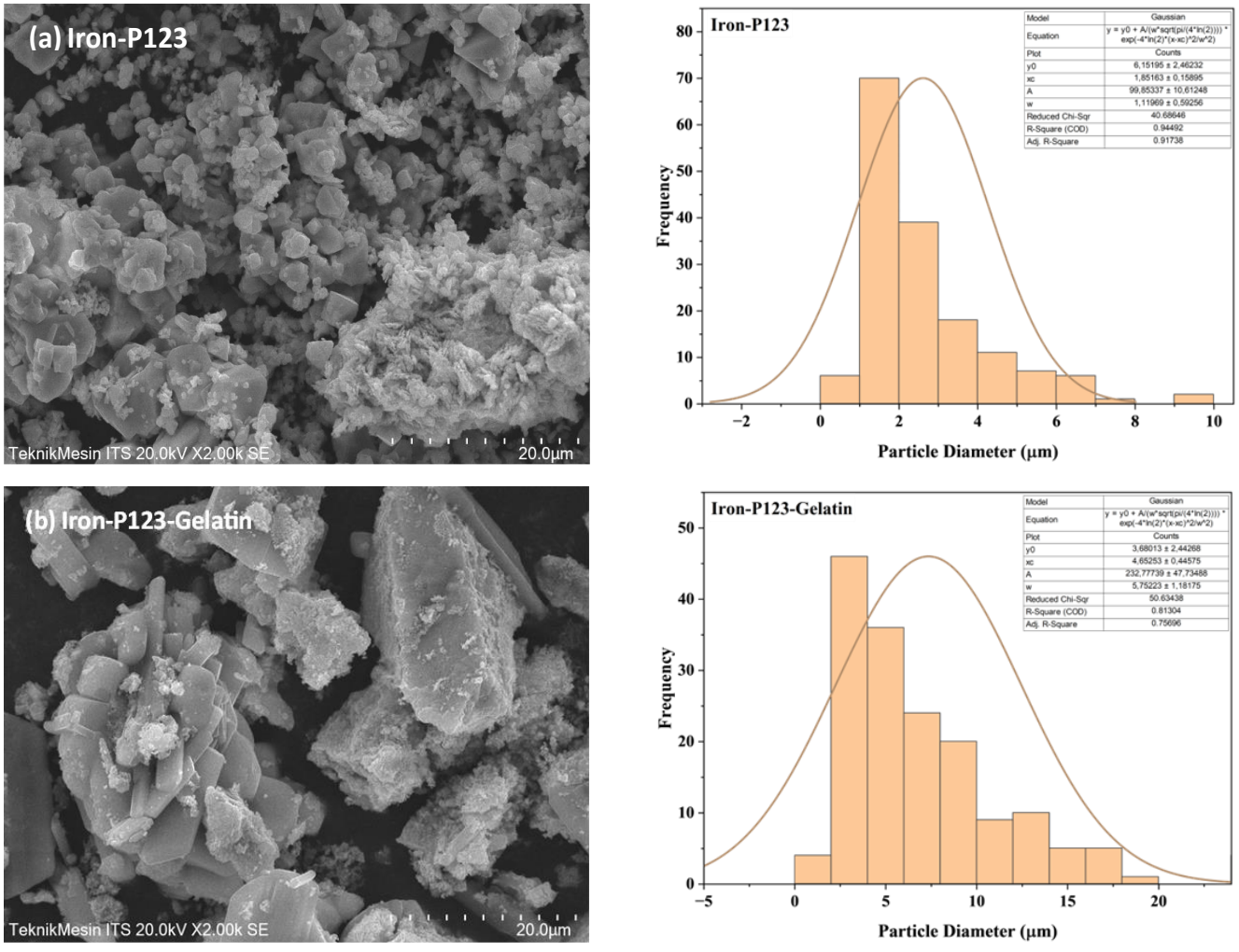

Figure 3. Morphology images and particle size distributions of iron oxide nanoparticles prepared with P123-gelatin and P123 templates.

Gelatin plays a prominent role in enhancing the pore size of iron oxide due to the strong affinity of its amine group to iron ions during synthesis. The porosity characteristics are favorable for active site exposure for the photodegradation process. Meanwhile, Table 2 presents the BET surface area, pore volume, and pore diameter of the samples with and without gelatin. It denotes that all values were significantly enhanced due to the addition of the gelatin template.

Figure 6 displays TGA curves of the iron oxide with and without gelatin, showing the link between temperature changes and sample weight loss. The pyrolysis process of iron was discovered to contain three stages of weight loss. The first stage occurs at the temperature range of 50 to 100 °C, the second stage is at 100 to 600 °C, and the third stage happens at 600 to 900 °C. The first and second stages are induced by reagent volatilization, sample dehydration, condensation, etc. The maximum weight loss rate from iron oxide with gelatin (iron-P123-gelatin) came at 100 to 600 °C. Here, the third stage was the stage responsible for the overall degeneration of the iron oxide with gelatin from 600 to 900 °C. The total weight loss of the iron-P123-gelatin was 19.39 g,

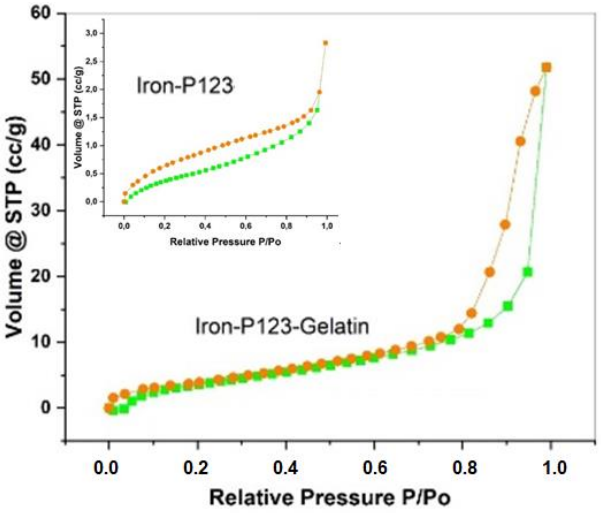

Figure 4. Nitrogen adsorption-desorption isotherms of iron-P123-gelatin and iron-P123 samples.

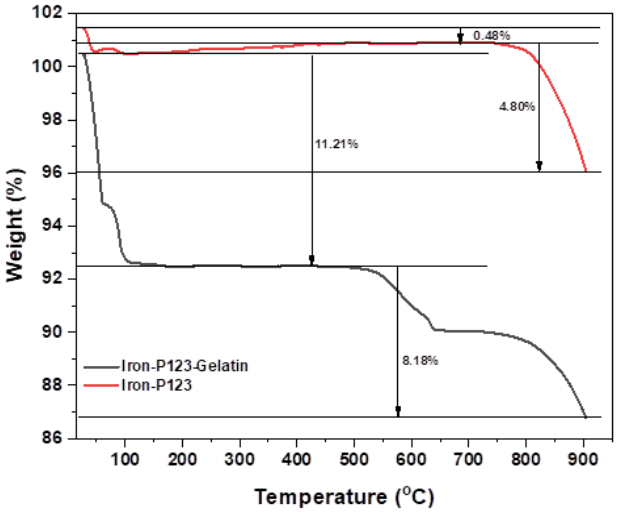

Figure 6. Thermal analysis of iron-P123-gelatin and iron-P123 samples.

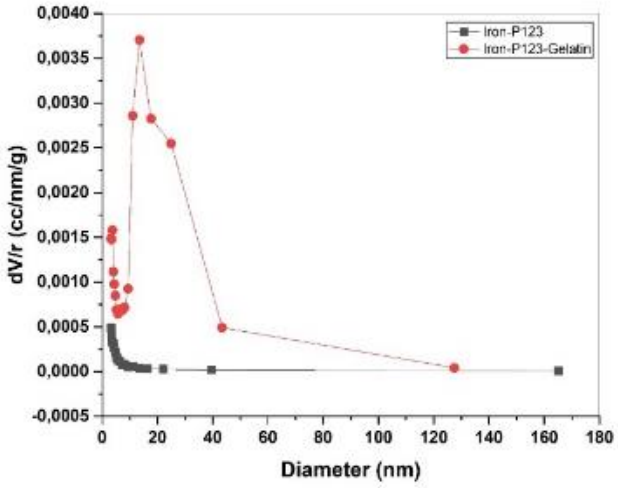

Figure 5. Pore size distribution of iron-P123-gelatin and iron-P123 samples.

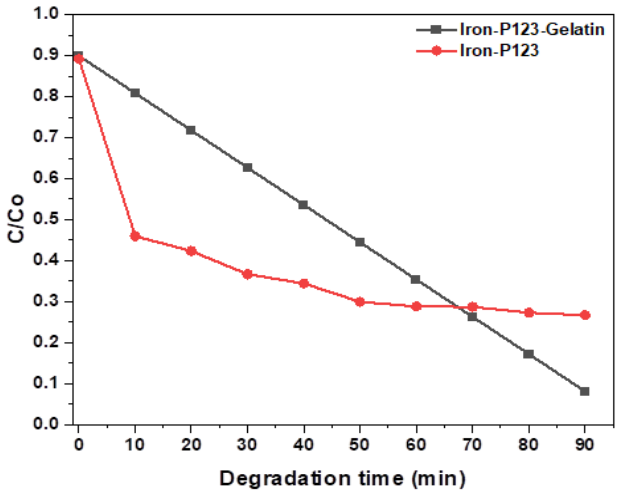

Figure 7. Photodegradation by iron-P123-gelatin and iron-P123 samples.

Table 2. Textural properties of the iron-P123-gelatin and iron-P123 samples.

Samples	Surface area (m^2/g)	Pore volume (cm^3/g)	Pore diameter (nm)
Iron-P123	1.70	0.004	3.2
Iron-P123-Gelatin	16.2	0.080	13.5

which was greater than that of iron-P123, 5.28%. This is considered because the carbon content of the iron-P123-gelatin was greater than that of iron-P123 due to the presence of gelatin.

The methylene blue degradation experiment was conducted with a continuous interval contact time of 10 to 90 min. Figure 7 displays the methylene blue deterioration against contact times. The degradation of methylene blue continuously increased from 10 to 90 min of contact time. Further, it reveals that the iron-P123-gelatin possessed nearly twice the photocatalytic activity than that of iron-P123. Thus, it can be inferred that the addition of gelatin, similar to combining double templates, can improve the effectiveness of photocatalytic degradation of the iron oxide nanoparticles because it can enhance the surface area and porosity.

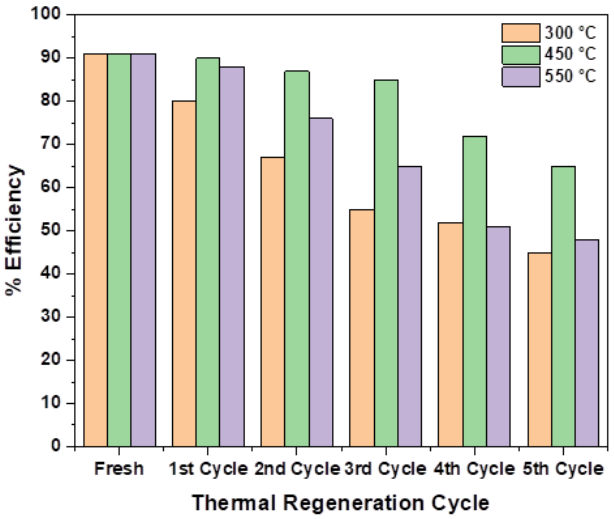

Figure 8. Thermal regeneration of methylene blue photodegradation of the iron-P123-gelatin sample.

Figure 8 and Table 3 show the thermal regeneration of methylene blue photodegradation of the iron-P123-gelatin sample carried out at various temperatures as many as 5 cycles. The total degradation efficiencies of the iron-P123-gelatin for 5 cycles at temperatures of 300, 450, and 550 °C were 390%, 490%, and 419%, respectively. It exhibits that the efficiency increased by 20% at 450 °C and declined by 14% when at 550 °C. From Figure 8, at all degradation temperatures, the degradation efficiency was reduced as there were more cycles. This is due to the degradation process, which leaves fewer methylene blue particles to be degraded in the next cycle.

Further, the increased temperature at 550 °C possessed a lower degradation efficiency compared to 450 °C. The high temperature has the possibility to completely decompose methylene blue and simultaneously damage the catalyst surface, causing the volume to shrinkage, thereby declining the photodegradation activity. From the results, it can be concluded that the temperature of 450 °C can be the ideal temperature for regenerating iron oxide synthesized using P123 and gelatin templates. However, 300 °C can be considered due to the insignificantly different efficiency achieved by the temperature.

The results of photodegradation and regeneration are an illustration of the potential for the iron samples in this research to be developed on a wide scale by considering polluted environmental conditions. Previous research reports (Table 4) on photocatalytic applications in

Table 3. Thermal regeneration of the iron-P123-gelatin sample.

Temperatures (°C)	% Efficiency per cycle						
	0	1st	2nd	3rd	4th	5th	Total
300	91	80	67	55	52	45	390
450	91	90	87	85	72	65	490
550	91	88	76	65	51	48	419

Table 4. pH effect on previous study on photodegradation of Methylene blue.

Sample	pH	% Efficiency	Ref
g-C_3N_4	5.0	57.0	[26]
g-C_3N_4	6.6	62.6	[26]
g-C_3N_4	8.0	72.7	[26]
g-C_3N_4	10.0	80.2	[26]
g-C_3N_4	11.0	98.7	[26]
Fe-P123-Gelatin	7.0	91.0	This work
$BaTiO_3/Bi_2WO_6$	1.1	98.0	[27]
$BaTiO_3/Bi_2WO_6$	6.4	80.0	[27]
$BaTiO_3/Bi_2WO_6$	13.0	49.0	[27]

photodegrading MB solutions at different pH environment can be a predictive image to measure the ability of iron-P123-gelatin to simulate dye wastewater as a model or real object in the environment. It is discovered by previoue research that the acidic–alkaline conditions have a significant impact on the methylene blue photodegradation and reach optimum in alkaline spot. In general, the iron samples in this investigation are expected to produce maximal photodegradation performance when utilized in a methylene blue solution at a pH of higher than 7.

$$\alpha\text{-}Fe_2O_3 + \gamma\text{-}Fe_2O_3 + h\upsilon \rightarrow Fe_2O_3\ (e^- + h^+) \quad (2)$$
$$OH^- + h^+ \rightarrow \cdot OH \quad (3)$$
$$H_2O + h^+ \rightarrow \cdot OH + H^+ \quad (4)$$
$$\cdot OH + \textit{methylene blue} \rightarrow CO_2 + H_2O \quad (5)$$
$$\textit{Methylene blue} + e^- \rightarrow CO_2 + H_2O \quad (6)$$

The study found that the degradation strength of methylene blue photocatalyst is significantly influenced by particle size, surface area, pore volume, thermal stability, and crystallinity. When light shines on the photocatalyst surface, electrons are promoted from the valence band to the conduction band, and radicals arise (Equation 2-6). Among all samples synthesized, iron-P123-Gelatin had a greater degradation percentage than samples synthesized from P123 alone. Iron samples synthesized with the P123-gelatin soft template were found to have a high surface area, crystallinity, and crystallite size, as well as large iron oxide particle sizes, all of which contribute to attracting species and increasing photoexcitation time by reducing recombination. The increased surface area and size of iron particles in the lattice provide more opportunities to attract methylene blue species, hence strengthening photodegradation. Furthermore, the sample crystal has hematite and maghemite phases, resulting in Fe^{2+} in the form of two distinct phases that can both take electrons due to possible positive Fe redox. As a result, Fe has a tendency to govern charge delivery and produce huge numbers of free radicals, increasing the photocatalytic activity of the doped photocatalyst. These free radicals target the methylene blue structure, causing progressive breakdown in a number of phases. Many of the intermediates generated during the disintegration of methylene blue are eventually transformed into simple degradation products, H_2O and CO_2. Aside from that, the high thermal stability due to the compact and solid structure of the multi-template self-assembly results from iron samples employing P123-Gelatin produces strong regeneration performance, with an optimum efficiency of 490% after 5 cycles. All of these findings demonstrate the tremendous potential for iron-P123-Gelatin to be developed on a big scale for the future management of aquatic waste.

4. Conclusion

Iron oxide nanoparticles as photocatalysts have been successfully synthesized using the sol-gel method and synthetic P123 and natural gelatin templates. Hematite and magnetite phases of iron oxide with and without gelatin where crystallinity and crystallize size of the iron-P123-gelatin sample enlarged due to the presence of gelatin as an attractant for Fe atomic particles. The formation was also validated with the FTIR spectra by revealing the Fe-O groups at about 500 cm^{-1} and the gelatin addition increased the intensity of the carboxyl and hydroxyl groups in the iron-P123-gelatin sample. Further, the BET surface area, pore volume, and pore diameter of the sample were also enlarged due to the gelatin addition. The sample also demonstrated a greater weight loss because of gelatin. Meanwhile, the photodegradation of methylene blue utilizing iron-P123-gelatin was much better than that of iron-P123 alone. Finally, the iron-P123-gelatin sample presented a good catalyst regeneration, and it is suggested that the ideal thermal regeneration temperature should be 450 °C.

Acknowledgments

The authors would like to thank Universitas Sebelas Maret, Indonesia, for their financial support of this work under the collaboration Internasional program. (Project No. 194.2/UN27.22/PT.01.03/2024 under Maria Ulfa)

CRediT Author Statement

Author Contributions: *M. Ulfa:* Conceptualization, Investigation, Resources, Data Curation, Methodology, Writing, Review and Editing, Supervision; S. D. Poetry: Methodology, Formal Analysis, Data Curation, Writing Draft Preparation; Data Validation. All authors have read and agreed to the published version of the manuscript.

References

[1] Essa, W.K., Yasin, S.A., Abdullah, A.H., Thalji, M.R., Saeed, I.A., Assiri, M.A., Chong, K.F., Ali, G.A.M. (2022). Taguchi L25 (5^4) Approach for Methylene Blue Removal by Polyethylene Terephthalate Nanofiber-Multi-Walled Carbon Nanotube Composite. *Water*, 14(8), 1242. DOI: 10.3390/w14081242.

[2] Lines, MG. (2008). Nanomaterials for practical functional uses. *Journal of Alloys and Compounds*, 449(1-2), 242-245. DOI: 10.1016/j.jallcom.2006.02.082.

[3] Safri, A., Fletcher, A.J. (2022). Effective Carbon/TiO(2) Gel for Enhanced Adsorption and Demonstrable Visible Light Driven Photocatalytic Performance. *Gels*, 8(4), 215. DOI: 10.3390/gels8040215.

[4] Gao, Z.-Z., Qi, N., Chen, W.-J., Zhao, H. (2022). Construction of hydroxyethyl cellulose/silica/graphitic carbon nitride solid foam for adsorption and photocatalytic degradation of dyes. *Arabian Journal of Chemistry*, 15(9), 104105. DOI: 10.1016/j.arabjc.2022.104105.

[5] Thi, T.P.T., Nguyen, D.T., Duong, T.Q., Luc, H.H., Vo, V. (2013). Facile Postsynthesis of N-Doped TiO2-SBA-15 and Its Photocatalytic Activity. *Advances in Materials Science and Engineering*, 2013, 638372. DOI: 10.1155/2013/638372.

[6] Ulfa, M., Anggreani, C.N., Sholeha, N.A. (2023). Fine-tuning mesoporous silica properties by a dual-template ratio as TiO2 support for dye photodegradation booster. *Heliyon*, 9(6), e16275. DOI: 10.1016/j.heliyon.2023.e16275.

[7] Kann, Y., Shurgalin, M., Krishnaswamy, R.K. (2014). FTIR spectroscopy for analysis of crystallinity of poly(3-hydroxybutyrate-co-4 -hydroxybutyrate) polymers and its utilization in evaluation of aging, orientation and composition. *Polymer Testing*, 40, 218-224. DOI: 10.1016/j.polymertesting.2014.09.009.

[8] Melzig, S., Niedbalka, D., Schilde, C., Kwade, A. (2018). Spray drying of amorphous ibuprofen nanoparticles for the production of granules with enhanced drug release. *Colloids and Surfaces A: Physicochemical and Engineering Aspects*, 536, 133-141. DOI: 10.1016/j.colsurfa.2017.07.028.

[9] Molinari, R., Lavorato, C., Argurio, P. (2017). Recent progress of photocatalytic membrane reactors in water treatment and in synthesis of organic compounds. A review. *Catalysis Today*, 281, 144-164. DOI: 10.1016/j.cattod.2016.06.047.

[10] Show, S., Chakraborty, P., Karmakar, B., Halder, G. (2021). Sorptive and microbial riddance of micro-pollutant ibuprofen from contaminated water: A state of the art review. *Science of The Total Environment*, 786, 147327. DOI: 10.1016/j.scitotenv.2021.147327.

[11] Zavala, M.A.L., Morales, S.A.L., Avila-Santos, M. (2017). Synthesis of stable TiO_2 nanotubes: effect of hydrothermal treatment, acid washing and annealing temperature. *Heliyon*, 3(11), e00456. DOI: 10.1016/j.heliyon.2017.e00456.

[12] McCarron, E., Chambers, G. (2021). A review of suitable analytical technology for physio-chemical characterisation of nanomaterials in the customs laboratory. *Talanta Open*, 4, 100069. DOI: 10.1016/j.talo.2021.100069.

[13] Mizuno, S., Yao, H. (2021). On the electronic transitions of α-Fe_2O_3 hematite nanoparticles with different size and morphology: Analysis by simultaneous deconvolution of UV–vis absorption and MCD spectra. *Journal of Magnetism and Magnetic Materials*, 517, 167389. DOI: 10.1016/j.jmmm.2020.167389.

[14] Sugrañez, R., Balbuena, J., Cruz-Yusta, M., Martín, F., Morales, J., Sánchez, L. (2015). Efficient behaviour of hematite towards the photocatalytic degradation of NO gases. *Applied Catalysis B: Environmental*, 165, 529-536. DOI: 10.1016/j.apcatb.2014.10.025.

[15] Ulfa, M., Prasetyoko, D., Bahruji, H., Nugraha, R.E. (2021). Green Synthesis of Hexagonal Hematite (alpha-Fe_2O_3) Flakes Using Pluronic F127-Gelatin Template for Adsorption and Photodegradation of Ibuprofen. *Materials*, 14(22), 6779. DOI: 10.3390/ma14226779.

[16] Mahlaule-Glory, L.M., Mapetla, S., Makofane, A., Mathipa, M.M., Hintsho-Mbita, N.C. (2022). Biosynthesis of iron oxide nanoparticles for the degradation of methylene blue dye, sulfisoxazole antibiotic and removal of bacteria from real water. *Heliyon*, 8(9), e10536. DOI: 10.1016/j.heliyon.2022.e10536.

[17] Abid, M.A., Abid, D.A., Aziz, W.J., Rashid, T.M. (2021). Iron oxide nanoparticles synthesized using garlic and onion peel extracts rapidly degrade methylene blue dye. *Physica B: Condensed Matter*, 622, 413277. DOI: 10.1016/j.physb.2021.413277.

[18] Kumar, S., Kumar, M., Singh, A. (2022). Synthesis and characterization of iron oxide nanoparticles (Fe_2O_3, Fe_3O_4): a brief review. *Contemporary Physics*, 62(3), 144-164. DOI: 10.1080/00107514.2022.2080910.

[19] Priya, P., Naveen, N., Kaur, K., Sidhu, A.K. (2021). Green Synthesis: An Eco-friendly Route for the Synthesis of Iron Oxide Nanoparticles. *Frontiers in Nanotechnology*, 3, 655062. DOI: 10.3389/fnano.2021.655062.

[20] Sharma, P., Holliger, N., Pfromm, P.H., Liu, B., Chikan, V. (2020). Size-Controlled Synthesis of Iron and Iron Oxide Nanoparticles by the Rapid Inductive Heating Method. *ACS Omega*, 5(31), 19853-19860. DOI: 10.1021/acsomega.0c02793.

[21] Parida, D., Salmeia, K.A., Sadeghpour, A., Zhao, S., Maurya, A.K., Assaf, K.I., Moreau, E., Pauer, R., Lehner, S., Jovic, M., Cordula, H., Gaan, S. (2021). Template-free synthesis of hybrid silica nanoparticle with functionalized mesostructure for efficient methylene blue removal. *Materials & Design*, 201, 109494. DOI: 10.1016/j.matdes.2021.109494.

[22] Ulfa, M., Prasetyoko, D., Bahruji, H., Nugraha, R.E. (2021). Green synthesis of Hexagonal Hematite (α-Fe_2O_3) flakes using Pluronic F127-Gelatin template for adsorption and photodegradation of ibuprofen. *Materials*, 14, 6779. DOI: 10.3390/ma14226779.

[23] Ulfa, M., Istanti, S.A. (2022). Synthesis of Mesoporous Silica Incorporated with Low Iron Concentration and Gelatin Co-Template via The Ultrasonication Method and Its Methylene Blue Photodegradation Performance. *Bulletin of Chemical Reaction Engineering & Catalysis*, 17(4), 831-838. DOI: 10.9767/bcrec.17.4.16210.831-838.

[24] Lee, S.-H., Kotal, M., Oh, J.-H., Sennu, P., Park, S.-H., Lee, Y.-S., Oh, I.-K. (2017). Nanohole-structured, iron oxide-decorated and gelatin-functionalized graphene for high rate and high capacity Li-Ion anode. *Carbon*, 119, 355-364. DOI: 10.1016/j.carbon.2017.04.031.

[25] Gomes, A.L.M., Andrade, P.H.M., Palhares, H.G., Dumont, M.R., Soares, D.C.F., Volkringer, C., Houmard, M., Nunes, E.H.M. (2021). Facile sol–gel synthesis of silica sorbents for the removal of organic pollutants from aqueous media. *Journal of Materials Research and Technology*, 15, 4580-4594. DOI: 10.1016/j.jmrt.2021.10.069.

[26] Paul, D.R., Sharma, R., Nehra, S.P., Sharma, A. (2019). Effect of calcination temperature, pH and catalyst loading on photodegradation efficiency of urea derived graphitic carbon nitride towards methylene blue dye solution. *RSC Advances*, 9(27), 15381–15391. DOI: 10.1039/c9ra02201e.

[27] Wang, Y., Sun, X., Xian, T., Liu, G., Yang, H. (2021). Photocatalytic purification of simulated dye wastewater in different pH environments by using $BaTiO_3/Bi_2WO_6$ heterojunction photocatalysts. *Optical Materials*, 113, 110853. DOI: 10.1016/j.optmat.2021.110853.